S. Afr. J. Chem., 2009, **62**, 67–76,
<http://journals.sabinet.co.za/sajchem/>.

The Effect of Synthesis Parameters on the Catalytic Synthesis of Multiwalled Carbon Nanotubes using Fe-Co/$CaCO_3$ Catalysts

Sabelo D. Mhlanga[a,b], Kartick C. Mondal[a,b], Robin Carter[a,b], Michael J. Witcomb[b,c] and Neil J. Coville[a,b]*

[a]*Molecular Sciences Institute and School of Chemistry, University of the Witwatersrand, Johannesburg, WITS 2050, South Africa.*

[b]*DST/NRF Centre of Excellence in Strong Materials, University of the Witwatersrand, Johannesburg, WITS 2050, South Africa.*

[c]*Microscopy and Microanalysis Unit, University of the Witwatersrand, Johannesburg, WITS 2050, South Africa.*

Received 17 December 2007, revised 22 December 2008, accepted 7 February 2009.

ABSTRACT

Fe-Co bimetallic catalysts supported on $CaCO_3$ were prepared by a wet impregnation, a deposition-precipitation and a reverse micelle method. The sizes of the Fe and Co particles were not affected by the Fe and Co sources (nitrate, acetate) when the wet impregnation and deposition-precipitation methods were used. 'Clean' multi-walled carbon nanotubes (MWCNTs) were obtained from all three Fe-Co synthesis procedures under optimal reaction conditions. The CNTs produced gave yields ranging from 623 % to 1215 % in 1 h under the optimal conditions, with similar outer diameters (o.d.) of 20–30 nm and inner diameters (i.d.) ~10 nm. The Fe/Co catalyst formed in the wet impregnation method revealed that the yield, diameter and purity of the CNTs were influenced by the C_2H_2/N_2 ratio, time and temperature. All the methods gave high-quality CNTs after short reaction times but the quality deteriorated as the synthesis time was increased from 5 to 360 min. Indeed, the most influential parameter in controlling CNT purity, length and o.d. was found to be the synthesis time. The as-synthesized CNTs were purified using a single-step mild acid treatment process (30 % HNO_3), which readily removed the support and metal particles.

KEYWORDS

Carbon nanotubes, synthesis, bimetallic catalyst, iron, cobalt.

1. Introduction

Since the synthesis of carbon nanotubes (CNTs) by Iijima in 1991,[1] methods to make these materials have been extensively investigated.[2] The synthesis of CNTs has sparked a worldwide escalation in research interest within the scientific community focussing on synthesis, modification or functionalization and application of these nanomaterials. The potential applications of CNTs are due to their outstanding mechanical and unique electrical properties.[3] Such applications include their use as chemical sensors, nanoconveyors, nanoelectronic devices, field emission sources, scanning probes and supports in catalysis.[3–5]

Several methods including arc discharge,[6,7] laser ablation,[8] pyrolysis[9] and chemical vapour deposition (plasma enhanced, thermal and catalytic) have been developed for the production of CNTs.[10,11] While all these methods seek to produce high-quality CNTs, the production of CNTs by the catalytic chemical vapour deposition (CCVD) method remains the prominent route for their large-scale production. This bottom-up approach of producing CNTs is favoured by the fact that it is a low-cost process that is versatile and results in relatively pure materials. Controlled growth of CNTs can be obtained through manipulation of the size of the nanoparticles that are used as catalysts in the CNT synthesis. The most widely used metals are Fe, Co and Ni as well as the alloys of these nanoparticles. The metals are usually supported on materials that are stable at high temperatures such as SiO_2, Al_2O_3, TiO_2 and zeolites.[12–16] However, purification of CNTs produced on these supports remains a challenge and requires several steps that result in damage to the CNT structures. Also, the solvents used during the purification process have to be disposed of to minimize environmental issues. To circumvent these problems, the use of readily removable supports (e.g. calcium carbonate) has been studied both by ourselves and others.[17–22]

Calcium carbonate ($CaCO_3$), albeit a low surface area material, has been shown to be a good support for the CCVD production of multiwalled carbon nanotubes (MWCNTs). At 700 °C, $CaCO_3$ changes to CaO (lime), which is an environmentally friendly material that can readily be dissolved in dilute acids such as HNO_3 and HCl. As a result, this support can be removed from the produced CNTs with ease, resulting in clean materials that are relatively free of contaminants.[17–22] It is also a cheap material that is readily available. The CNTs produced on $CaCO_3$ have been used as supports for catalysts in the Fischer-Tropsch reaction[19] and for the thermal decomposition of hydrocarbons.[23]

The investigation of CNT synthesis over metals supported on silica and alumina has been actively studied and factors that affect the catalytic activity and ultimately the structure of the CNTs produced have been determined.[24–28] In contrast, the behaviour of metals supported on $CaCO_3$ for CNT production has been little studied.[17–22,29,30]

Kathyayini *et al.*[18] studied the activity of Fe, Co and Fe-Co supported on Ca and Mg oxides, hydroxides and carbonates for the synthesis of CNTs. Their catalyst-support mixtures were prepared by the wet impregnation method and the study revealed that Fe-Co supported catalysts gave the best activity. The excellent activity was achieved by favourable metal-support interactions, which greatly influenced the CNT selectively. Cheng *et al.*[20] recently reported on the use of $CaCO_3$ nanocrystals as a catalyst support for the CVD synthesis of CNTs. The

* To whom correspondence should be addressed. E-mail: neil.coville@wits.ac.za.

catalyst-support mixtures were also prepared by the wet impregnation method and the authors observed that the nanocrystalline $CaCO_3$ produced high yields of CNTs.

Magrez *et al.*[21] reported on a systematic study of the effect of catalyst composition, catalyst carrier and synthesis time on the yield and quality of CNTs grown by CCVD. The study revealed that the carbon yield is influenced by the catalyst composition Fe/Co mixtures and that maximum yield is obtained at a Fe:Co ratio of about 2:1. They also reported on the carbon yield obtained from the catalysts after different synthesis times (2–100 min), showing that maximum CNT growth occurred between 2 and 30 min; no clear variation in the length or in the outer diameter of CNTs was observed within this growth time. The presence of CO_2 in the system was also proposed to assist in the formation of CNTs.[22]

Schmitt *et al.*[30] observed that $CaCO_3$ decomposed into CaO and CO_2 at high temperature and in so doing gave catalyst particles with outer diameters belonging to two main groups with sizes of 8–35 nm and 40–60 nm, respectively. Dervishi *et al.*[29] also reported on the synthesis of MWCNTs on a $CaCO_3$ supported Fe-Co catalyst. They observed that the outer diameter of the MWCNT products obtained fell into two groups; one associated with growth on Fe-Co/CaO and the other with growth on Fe-Co/$CaCO_3$. Finally See *et al.*[31] have reported on the high-yield synthesis of MWCNTs on Fe-Co catalysts supported on a $CaCO_3$ substrate using a fluidized bed reactor.

In all the reported studies, catalyst-support mixtures were prepared by impregnation methods using different sources of carbon (e.g. acetylene and ethylene) and different carrier gases (e.g. argon and nitrogen). Similar MWCNT products were obtained from all studies but the products had a varied diameter distribution.

In this study we have investigated factors that affect the morphology of the CNTs, in particular using an Fe-Co/$CaCO_3$ catalyst prepared by the wet impregnation method. This study revealed the key role of reaction time on both CNT quantity and quality. We show, by means of TEM, that as the synthesis time is increased, carbon continues to deposit on the already formed CNTs resulting in the thickening and destruction of the CNTs.[33] To explore the Fe-Co/$CaCO_3$ catalysts further, an investigation of the effect of the catalyst preparation route and the catalyst counter-ion on the synthesis of CNTs was undertaken. To this end, the synthesis strategy was to produce CNTs with similar diameters from different routes. In this work this was achieved by preparing catalysts using wet impregnation, deposition-precipitation and water-in-oil microemulsion (reverse micelles) methods.[32]

2. Experimental

2.1. Preparation of Catalysts

2.1.1. *Wet Impregnation*

$Fe(NO_3)_3{\cdot}9H_2O$, $Co(NO_3)_2{\cdot}6H_2O$, $Fe(CH_3CO_2)_2$ and $Co(CH_3CO_2)_2$ (Sigma-Aldrich, St Louis, MO, USA) were used to prepare the different catalysts. Calculated amounts of the Fe and Co nitrates were mixed, ground to a fine powder and dissolved in distilled water to make a 0.3 mol L^{-1} Fe-Co (50:50 m/m) precursor solution. A similar Fe-Co acetate precursor solution was made from the metal acetates. This solution (28 mL) was added to the $CaCO_3$ support (10 g) and the mixture was left to stir for 30 min. The metal-support mixture was then filtered and the insoluble product was dried in an air oven at 120 °C for 12 h, cooled to room temperature, ground and finally screened through a 150 μm sieve. The catalyst powder was then calcined at 400 °C for 16 h in a static air oven. The 5 % metal-loaded catalysts were named IMPN (prepared from nitrate solution) and IMPA (prepared from acetate solution).

2.1.2. *Deposition-precipitation*

The $CaCO_3$ support was stirred in distilled water (100 mL) for 5 min. An aqueous 0.3 mol L^{-1} solution (28 mL) of the catalyst precursor was added dropwise to the stirred $CaCO_3$ slurry and the mixture left to stir for another 5 min. Ammonium hydroxide (12.5 %) was then added dropwise to the slurry and when the pH reached 7.2 the mixture was left to stir for another 10 min. The resulting metal-support mixture was then filtered and dried in an oven at 120 °C for 12 h, cooled to room temperature and then ground and screened through a 150 μm sieve. The total loading of the Fe-Co catalysts on the $CaCO_3$ was 5 mass %. The material was then calcined at 400 °C for 16 h in static air. The catalysts prepared from the nitrate and acetate Fe/Co precursor solution were labelled DPN and DPA, respectively.

2.1.3. *Reverse Micelles*

Isooctane, n-butanol, sodium borohydride ($NaBH_4$) and cetyl-trimethyl-ammonium-bromide (CTAB) were purchased from Sigma-Aldrich and were used as received. CTAB and n-butanol were used as the surfactant and co-surfactant molecules, respectively. Isooctane was used as the oil phase while distilled water was used as the aqueous phase. $NaBH_4$ was added to the aqueous solution to reduce the metals under a N_2 flow.[32] $Fe(NO_3)_3{\cdot}9H_2O$ and $Co(NO_3)_2{\cdot}6H_2O$ were used as the Fe and Co sources.

Two microemulsions were prepared (Fig. 1). Microemulsion A consisted of an aqueous solution containing Fe^{3+} (0.3 mol L^{-1}) and Co^{2+} (0.3 mol L^{-1}) ions obtained by dissolving $Fe(NO_3)_3{\cdot}9H_2O$ and $Co(NO_3)_2{\cdot}6H_2O$ in 14 mL distilled water. This was added to a mixture containing 20 mL of isooctane, 5 mL of n-butanol and 0.46 g of CTAB. The microemulsion was stirred vigorously for 10 min. Microemulsion B consisted of a solution of $NaBH_4$ (14 mL, 0.5 mol L^{-1}) and CTAB (0.46 g), n-butanol (5 mL) and isooctane (20 mL). The microemulsion was stirred vigorously for 10 min.

Microemulsion B was then slowly added to microemulsion A using ultrasonic agitation for 90 min under a continuous N_2 flow to minimize oxidation. The solution immediately turned black after the two microemulsions were mixed, due to the formation of metallic Fe and Co in the micelles. The micelle solution was then disrupted with an excess of ethanol (150 mL) and centrifuged. The precipitate was repeatedly washed with methanol to remove the surfactant. The resulting powder, which was dark brown in colour, was dried at 100 °C for 12 h in an air oven. It was then calcined at 600 °C to obtain the crystalline nanoparticles, which were then deposited on the $CaCO_3$ support using ethanol to give a 5 mass % Fe-Co/$CaCO_3$ catalyst. The catalyst prepared was labelled as RM.

2.2. Carbon Nanotube Synthesis

CNTs were synthesized by the decomposition of acetylene (C_2H_2) (Afrox) in a tubular quartz reactor (51 cm × 1.9 cm i.d.) that was placed horizontally in a furnace. The furnace was electronically controlled such that the heating rate, reaction temperature and gas flow rates could be accurately maintained as desired. The catalyst (0.2 g) was spread to form a thin layer in a quartz boat (120 mm × 15 mm) and the boat was then placed in the centre of the quartz tube. The furnace was then heated at 10 °C min^{-1} under flowing N_2 (40 mL min^{-1}). Once the temperature had

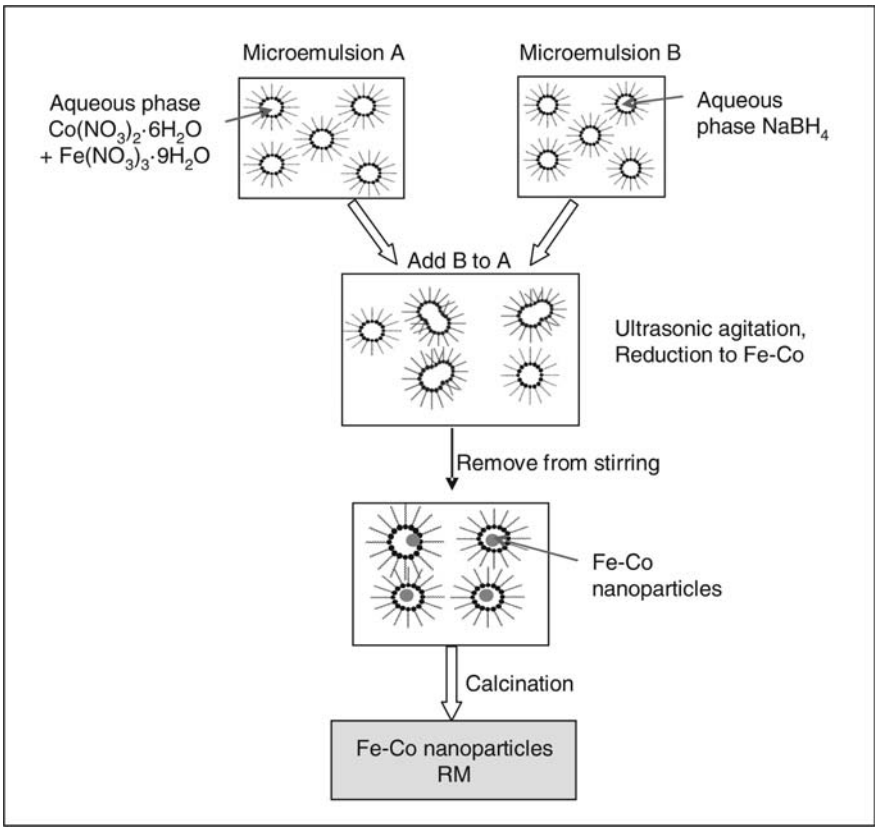

Figure 1 The synthetic pathway for the preparation of Fe-Co nanoparticles using reverse micelles.

reached 700 °C, the N_2 flow rate was set to 240 mL min^{-1} and C_2H_2 was introduced at a constant flow rate of 90 mL min^{-1}. After 60 min of reaction time, the C_2H_2 flow was stopped and the furnace was left to cool down to room temperature under a continuous flow of N_2 (40 mL min^{-1}). The boat was then removed from the reactor and the carbon deposit that formed along with the catalyst was weighed.

2.3. Characterization of Catalysts and CNTs

The Fe-Co catalysts supported on $CaCO_3$ were characterized by a range of techniques. The morphology of the support was characterized by transmission electron microscopy (TEM) (JEOL 100S Electron Microscope, Tokyo, Japan), while the size and distribution of the Fe-Co nanoparticles were determined at higher magnification using a Philips CM200 (Philips, Eindhoven, The Netherlands) equipped with a Gatan Imaging Filter. For TEM observation, the samples were sonicated in ethanol for 10 min and thereafter deposited on a holey carbon-coated TEM Cu grid. Energy dispersive X-ray spectroscopy (EDX) and powder X-ray spectroscopy (PXRD) were used to confirm the elemental composition of the Fe-Co bimetallic nanoparticles. The metal loading (mass %) on the support was confirmed by inductively coupled plasma–atomic emission spectrometry (ICP-AES) measurements using semiconductor detectors (CCD) and by quantitative TGA using a Perkin-Elmer Pyris 1 TGA (Perkin-Elmer, Waltham, MA, USA). The total surface area and porosity of the catalysts were ascertained using a Micromeritics TriStar Surface Area and Porosity Analyzer (Micromeritics Instrument Corp., Norcross, GA, USA). A slight variation (within error bar) on the diameter distribution of the MWCNTs was observed within each sample as well as with the different catalysts used. Carbon nanotube structures and size distributions were ascertained from TEM studies.

The percentage carbon deposit (% C) was determined as described elsewhere.[18] In the calculation it was assumed that all $CaCO_3$ was converted to CaO.[29,30] The selectivity of the catalysts was determined based on the different forms of carbon materials produced *before purification* of the product. TEM was used to distinguish the CNTs from other carbonaceous products (e.g. carbon spheres and carbon nanofibres) that were formed along with the CNTs under non-ideal reaction conditions. Under the optimal reaction conditions the selectivity towards CNTs was close to 100 %. The percentage selectivity was determined using counting procedures, i.e. by literally counting images in no fewer than 25 TEM photographs. Under non-optimal conditions spheres also formed. Long reaction times at T = 700 °C resulted in tube thickening and tube shortening. Thus, product selectivity to CNT formation at t > 2 h was determined by measuring and counting the tube fragments.

The properties of the CNTs observed under TEM were also confirmed by Raman spectroscopy (J-Y T64000 micro-Raman spectrometer, Horiba Jobin-Yvon, Ltd., Stanmore, UK) equipped with a liquid nitrogen cooled charge coupled device detector. All samples were measured after excitation with a laser wavelength of 514.5 nm. The CaO and residual Fe-Co particles in the product were removed by stirring the products in 30 % HNO_3 for at least 30 min at room temperature. The acid-treated CNTs were then washed with distilled water until the washings were neutral. The purification of CNTs was monitored by TEM, TGA and PXRD (Bruker AXS D8 Advance PXRD, Bruker South Africa (Pty.) Ltd., Cramerview, SA).

3. Results and Discussion

3.1. Analysis of the Catalyst

The surface area of commercial $CaCO_3$ was found to be about 10 $m^2 g^{-1}$. The Fe-Co/$CaCO_3$ materials also possess similar surface areas (Table 1). The freshly prepared supported catalysts were

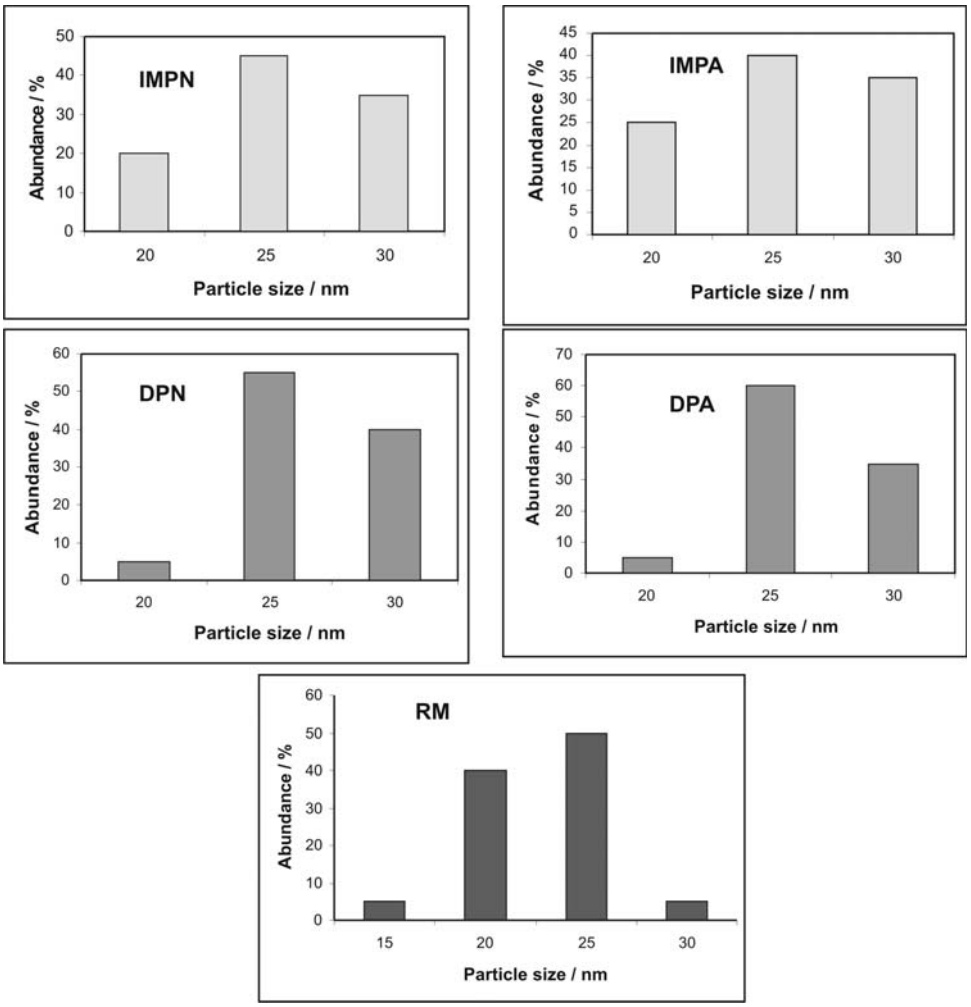

Figure 2 Diameter distribution of the Fe-Co particles prepared by the IMP, DP and RM methods.

heated under normal carbon nanotube synthesis conditions (t = 60 min, T = 700 °C) in N_2 (240 mL min^{-1}) but in the absence of the carbon source (C_2H_2). It was observed that the surface areas of the support and catalysts almost doubled within an hour when subjected to the reaction conditions in the absence of C_2H_2. This result is due to the decomposition reaction $CaCO_3 \rightarrow CaO + CO_2$ that occurs at 700 °C.[22] When the supported catalysts were further heated at 700 °C for up to 2 h, the surface area of the supported catalyst did not increase any further.

In this study, the dispersion of the metal particles on the support prior to heating to 700 °C could not be effectively studied by electron microscopy as the $CaCO_3$ decomposed under the electron beam. TEM analysis of the Fe-Co/$CaCO_3$ prepared by the three synthesis procedures (wet impregnation, deposition-precipitation and reverse micelles) after heating to 700 °C for 1 h in N_2, but prior to CNT synthesis, revealed that the metal particles were all ~ 20–30 nm in diameter (Fig. 2). Some variation in particle sizes within the 20–30 nm range was observed for the different methods used. In particular the RM samples gave on average smaller particles in the 20–30 nm range. This effect did not however impact on the parametric studies that were performed. The source of the catalyst (i.e. whether nitrate or acetate) also did not influence the Fe-Co particle size when either the IMP or DPN methods were used. HRTEM revealed the presence of lattice-fringe patterns (~0.2 nm apart), displaying the highly crystalline nature of the nanoparticles.

Energy dispersive X-ray spectroscopy (EDX) revealed that all particles contained both Fe and Co in a close to 1:1 mass % ratio in all the individual particles that were analyzed. An example of a TEM image of the Fe-Co on $CaCO_3$ catalyst prepared by the impregnation process is shown in Fig. 3 (see Supplementary Material Fig. S1 for EDX data).

Table 1 Surface areas of $CaCO_3$ and supported catalysts before and after heating at 700 °C under N_2 (300 mL min^{-1}).

Sample identification	BET surface area before heating /m^2 g^{-1} [a]	BET surface area after heating for 60 min /m^2 g^{-1} [a]
$CaCO_3$ support	9.6	22.3
IMPN	10.8	18.2
IMPA	11.5	22.6
DPN	13.6	22.5
DPA	10.6	19.4
RM	10.3	21.4

[a] ±5 %

3.2. Catalytic Reactions

Experiments were carried out under conditions found to be optimal to produce CNTs (i.e. ratio = 1:3 or 90 mL min^{-1} C_2H_2:240 mL min^{-1} N_2) which involved passage of the gas mixture over the $CaCO_3$ (no metal) at 700 °C. TEM analysis of samples taken at different times (0.5 h, 1 h, 3 h and 6 h) revealed that no carbon nanotubes were formed. The TEM images revealed that after 1 h, the support was still well dispersed.

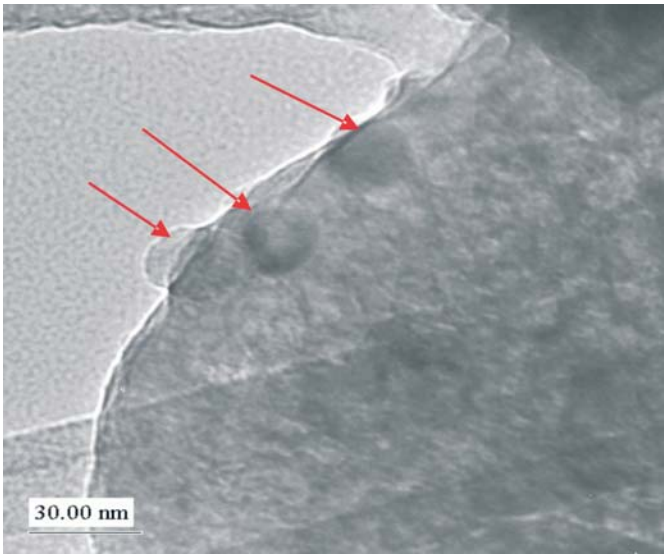

Figure 3 TEM image of IMPN. Arrows show some Fe-Co nanoparticles (~30 nm) supported on $CaCO_3$ after calcination.

Further, the surface area of the support initially increased and then remained unchanged from 30 to 120 min (22.3 $m^2 g^{-1}$). However, after 6 h of reaction time, the support appeared to have sintered and now had a low surface area (4.0 $m^2 g^{-1}$) (see Supplementary Material Fig. S2). These observations reveal that $CaCO_3$/CaO at 700 °C is stable under the reaction conditions for $t < 2$ h and is suitable for the synthesis of CNTs.[18]

The effect of catalyst particle size on CNT production is now well established.[26,34] This also applies to catalyzed reactions performed over $CaCO_3$.[35] Further, studies have also shown that Fe-Co bimetallic catalysts are more effective than either Fe or Co catalysts when supported on $CaCO_3$.[18,20–22,29,30] We have chosen to prepare a 50:50 Fe-Co catalyst as our studies indicated good activity for this mixture (see Supplementary Material Fig. S3), although some authors have suggested that a 2:1 Fe-Co catalyst may be even more active.[21,29]

While some work has previously been reported on the effect of reaction conditions on the synthesis of CNTs using $CaCO_3$ as a substrate, in this work we have investigated (i) the effect of the catalyst synthesis process on the CNT yield and quality (using about the same sized metal particles) and (ii) three reaction parameters, namely C_2H_2/N_2 ratio, temperature and time on stream (synthesis time), on the formation of CNTs.

3.2.1. *Effect of Catalyst Preparation Method*

We chose to synthesize CNTs from Fe-Co catalysts prepared by three routes and with different sources of Fe and Co. Conditions were chosen to keep the particle sizes approximately the same (20–30 nm). Figure 4 shows TEM images of the CNTs produced from the IMPN, DPN and RM methods. The images reveal that all the CNTs are multiwalled in nature with a random (spaghetti-like) orientation. Analysis of the CNTs using TEM (Fig. 4d) revealed that all the CNTs had defects in the graphite tubes and the degree of disorder was similar for all the CNTs. TEM analysis indicated that the CNTs produced using the three different preparation methods contained no catalyst particles in their tips and little residual metal inside their tube cavities. Thus the synthesized CNTs form *via* a base-growth mode involving a strong interaction between Co-Fe metal particles and the CaO.[25]

Figure 5 shows a graphical representation of the percentage carbon deposit obtained from the different catalysts and the amounts of MWCNTs produced at different temperatures. Gas

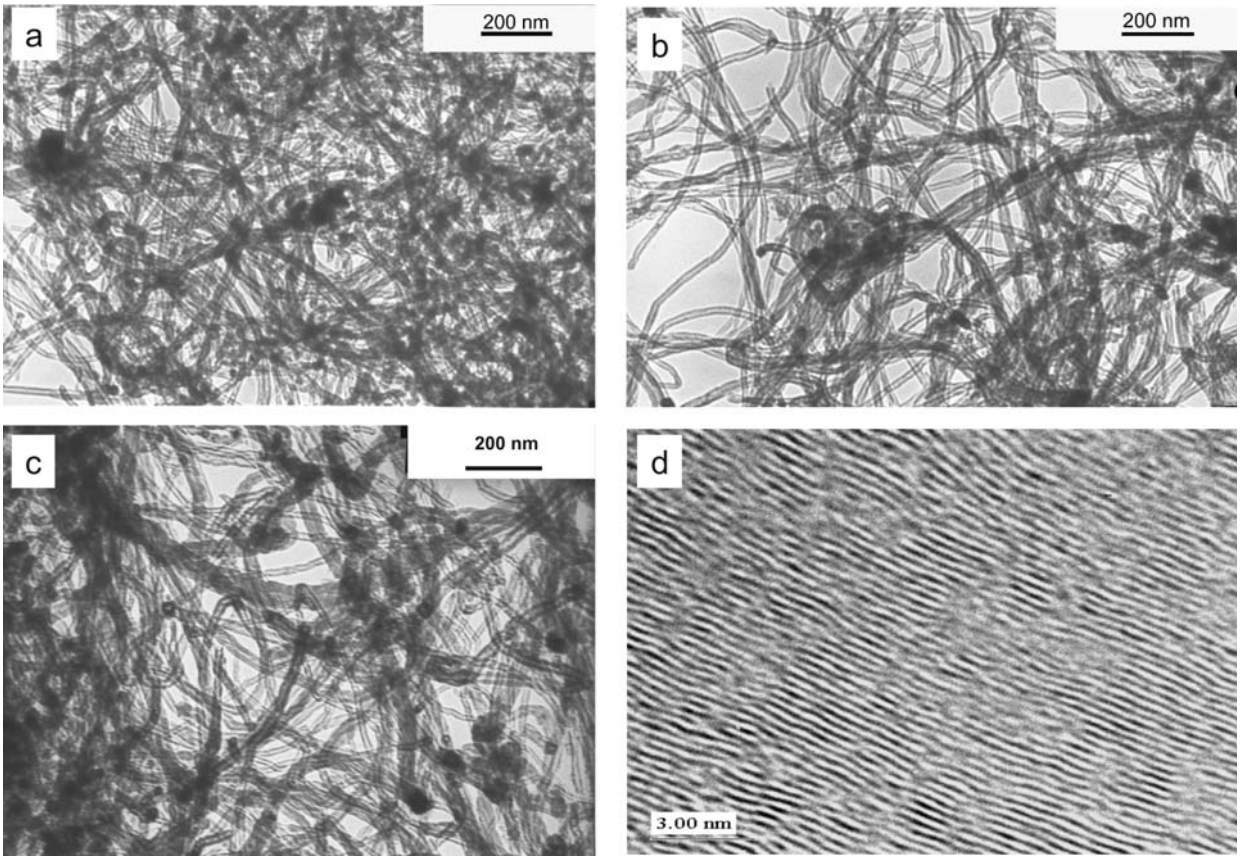

Figure 4 TEM images of MWCNTs prepared by the (**a**) IMPN, (**b**) DPN, (**c**) RM methods and (**d**) a general higher magnification TEM image showing a much closer look at the 'wavy-like' 0.34 nm (0002) graphite lattice fringes of the CNTs.

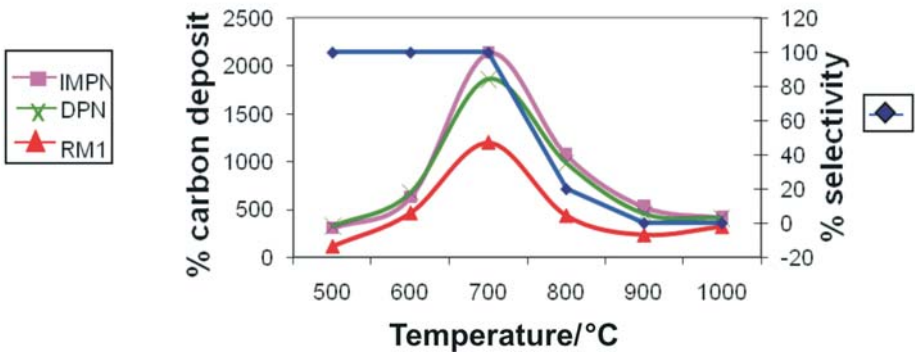

Figure 5 Graph showing the amount of CNTs produced and the percentage selectivity at different reaction temperatures in the CVD of C_2H_2 diluted with N_2 (C_2H_2:N_2 = 1:3, t = 1 h). The selectivity profile is similar for all the supported catalysts.

flow rates were kept fixed (C_2H_2 = 90 mL min^{-1}, N_2 = 240 mL min^{-1}) for each experiment. The reaction time was 60 min and 0.2 g of catalyst was used in each experiment. The data indicate that the best temperature to produce MWCNTs using a 5 mass % Fe-Co/$CaCO_3$ catalyst is 700 °C. At this temperature, all the catalysts show excellent selectivity (~100 %) towards MWCNTs. The yields of MWCNTs obtained were relatively high for the IMPN and DPN catalysts. Lower yields of MWCNTs were obtained with the RM catalysts. The cause of the difference in the amount of carbon deposit produced is unknown and was not explored further.

Raman spectroscopic analysis was also used to characterize the CNTs. Two peaks at 1344 cm^{-1} and 1574 cm^{-1} corresponding to the disorder-induced band (D band) and the Raman-allowed tangential mode (G band) were observed.[36] The D mode indicates the disorder features of the carbon while the G mode is associated with the ordered graphite in the CNTs.[36] A small shoulder on the G band corresponding to the D band was observed at 1615 cm^{-1}. The intensity ratio of the D band to the G band (I_D/I_G) was found to be ~0.7 for all the CNTs, suggesting similar structures for the CNT samples.

3.2.2. *Effect of Carbon Source Dilution*

The effect of dilution of the carbon source by N_2 on the activity and selectivity of 5 mass % Fe, 5 mass % Co and 5 mass % Fe-Co/$CaCO_3$ supported catalysts is shown in Fig. 6. This study was performed on catalysts that were prepared by the wet impregnation method. The study was carried out at 700 °C for 1 h. A total gas flow rate of 330 mL min^{-1} was used in all experiments. The ratio of C_2H_2 to N_2 was changed from 1:10 (i.e. 30 mL min^{-1} C_2H_2 and 300 mL min^{-1} N_2) to 1:0 (330 mL min^{-1} C_2H_2 and no N_2).

Figure 6 reveals:

- The order of activity is Fe-Co > Co > Fe.
- When the flow rate ratio of C_2H_2 to N_2 was changed from 1:10 to ~1:3 the CNT yield also increased for all the catalysts. In every case the selectivity to CNTs was ~100 % (Fig. 7a).
- The maximum % C obtained with ~100 % selectivity to CNTs was 1215 % using a Co-Fe catalyst. This was obtained when the flow rate ratio of C_2H_2 to N_2 was 90 mL min^{-1} C_2H_2 and 240 mL min^{-1} N_2 (~1:3).
- When the ratio of C_2H_2 to N_2 was greater than 1:2.67, the product contained a mixture of CNTs, carbon microspheres (CMSs) and nanofibres (Fig. 7b).
- When the carbon source was not diluted (i.e. 100 % C_2H_2), the product contained only carbon microspheres and a few nanofibres (Fig. 7c).
- The inner diameters of the CNTs as well as the lengths were not affected by the C_2H_2/N_2 ratio. About 90 % of the tubes have inner diameters within 5–10 nm and outer diameters (o.d.) within 15–30 nm for the C_2H_2/N_2 ratios that were used. However a small variation in the CNT outer diameter was observed. The o.d. increases slightly with increase in the C_2H_2 concentration.

Significant yields of accreted CMSs were observed, when the reaction conditions did not favour CNT formation (i.e. when

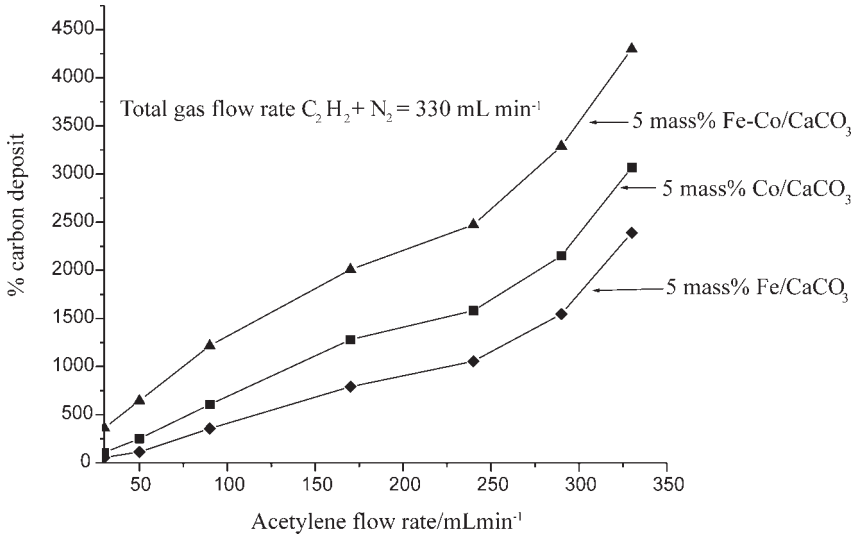

Figure 6 A graph showing percentage C obtained by varying the gas flow ratio of C_2H_2 to N_2. The synthesis time was 1 h for all reactions and the reaction temperature was 700 °C.

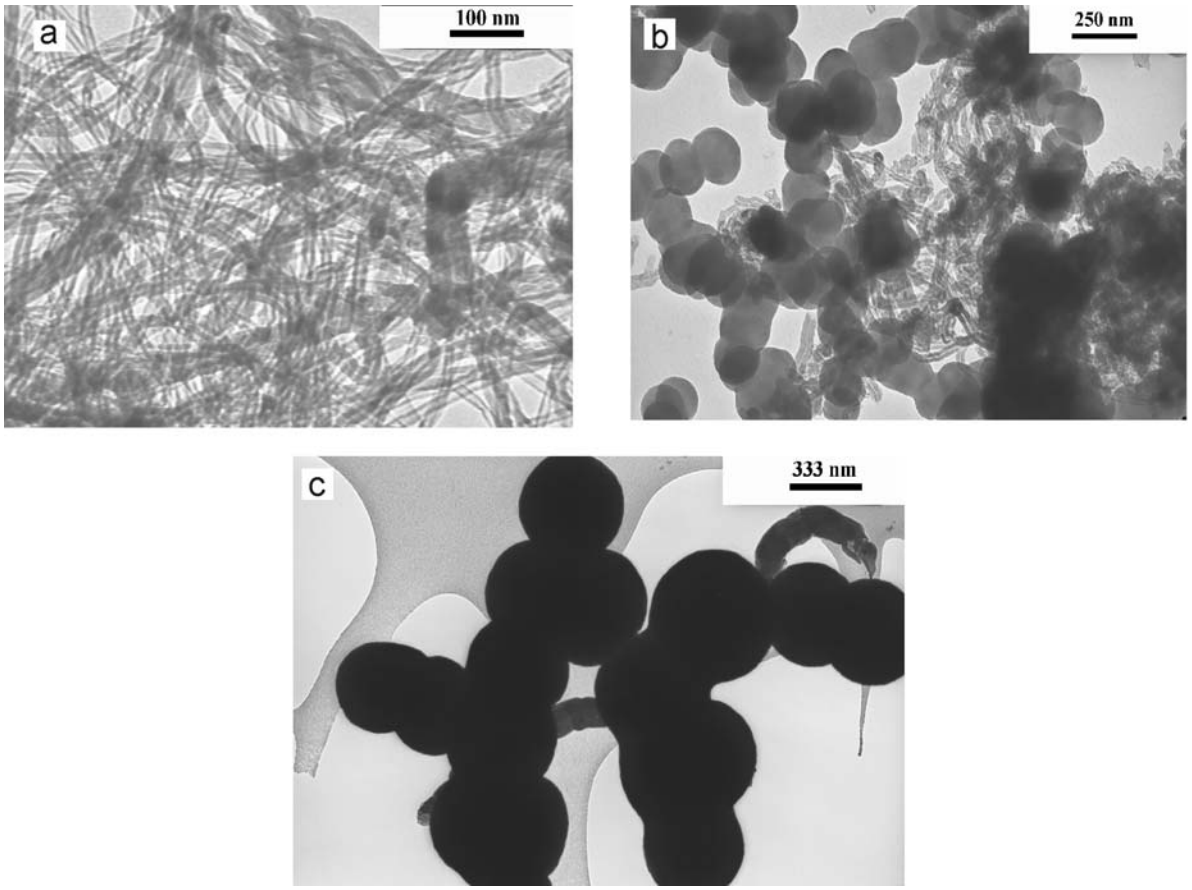

Figure 7 Low magnification TEM images of the carbon deposit produced with different dilution ratios of feedstock gases: (**a**) C_2H_2:N_2 = 1:2.7 (100 % CNTs), (**b**) C_2H_2:N_2 = 1:1 (CNTs and CMSs), (**c**) pure C_2H_2 (CMSs and CNFs); T = 700 °C, t = 1 h.

C_2H_2:N_2 > 1:2.67). TEM analysis revealed that the carbon microspheres are round, smooth, clean, solid and did not show large porosity.[37,38] We attribute the formation of these CMSs to the direct pyrolysis of the C_2H_2 that occurs without intervention of a catalyst *via* a mechanism similar to the acetylene black process.[39] This proposal is supported by the observation that CMS formation was observed when $CaCO_3$ containing no catalyst was used. In conclusion the dilution of the carbon source (C_2H_2) with N_2 significantly affects the product yield and the selectivity of the catalysts towards CNT formation.[17,18,20–22,29,30]

3.4. Effect of Time on Stream (TOS)

Experiments were performed to investigate the effect of reaction time on catalyst activity and the types of products formed. The study was undertaken on the catalysts synthesized by the wet impregnation method. The reaction temperature was fixed at 700 °C and the flow rates used were: C_2H_2 = 90 mL min^{-1}, N_2 = 240 mL min^{-1} in all experiments. The product yield, as expected, was found to increase as the reaction time was increased from 15 to 360 min (Fig. 8). The reaction was also monitored by TEM. The TEM studies revealed that both the diameters and the lengths of the products varied with reaction time. TEM images for the CNTs produced from the IMPN catalyst after different times are shown in Fig. 9.

After 1 h the product comprised long multiwalled CNTs with outer diameters of 20–30 nm (Fig. 9b). These CNTs were spongy in texture and very light. CNTs measured after 2.5 h were short with a rough surface and their outer walls had thickened

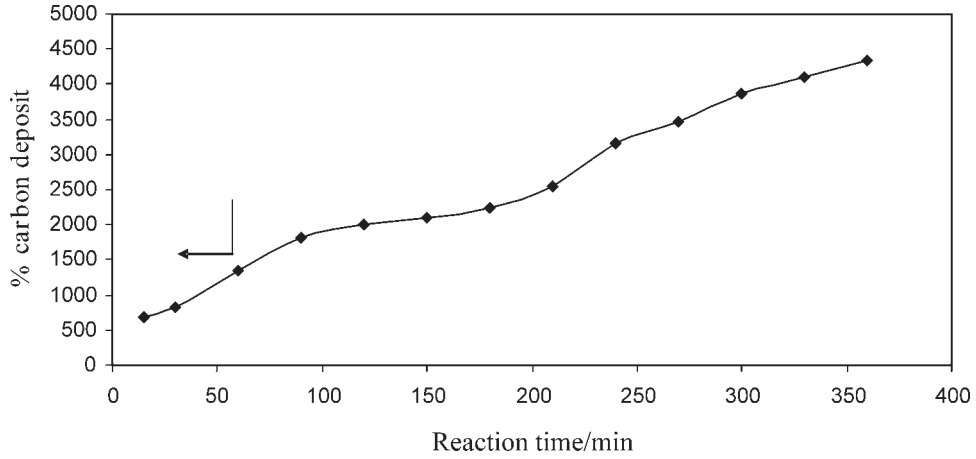

Figure 8 Graph showing the amounts of CNTs produced after different reaction times using IMPN catalysts (T = 700 °C).

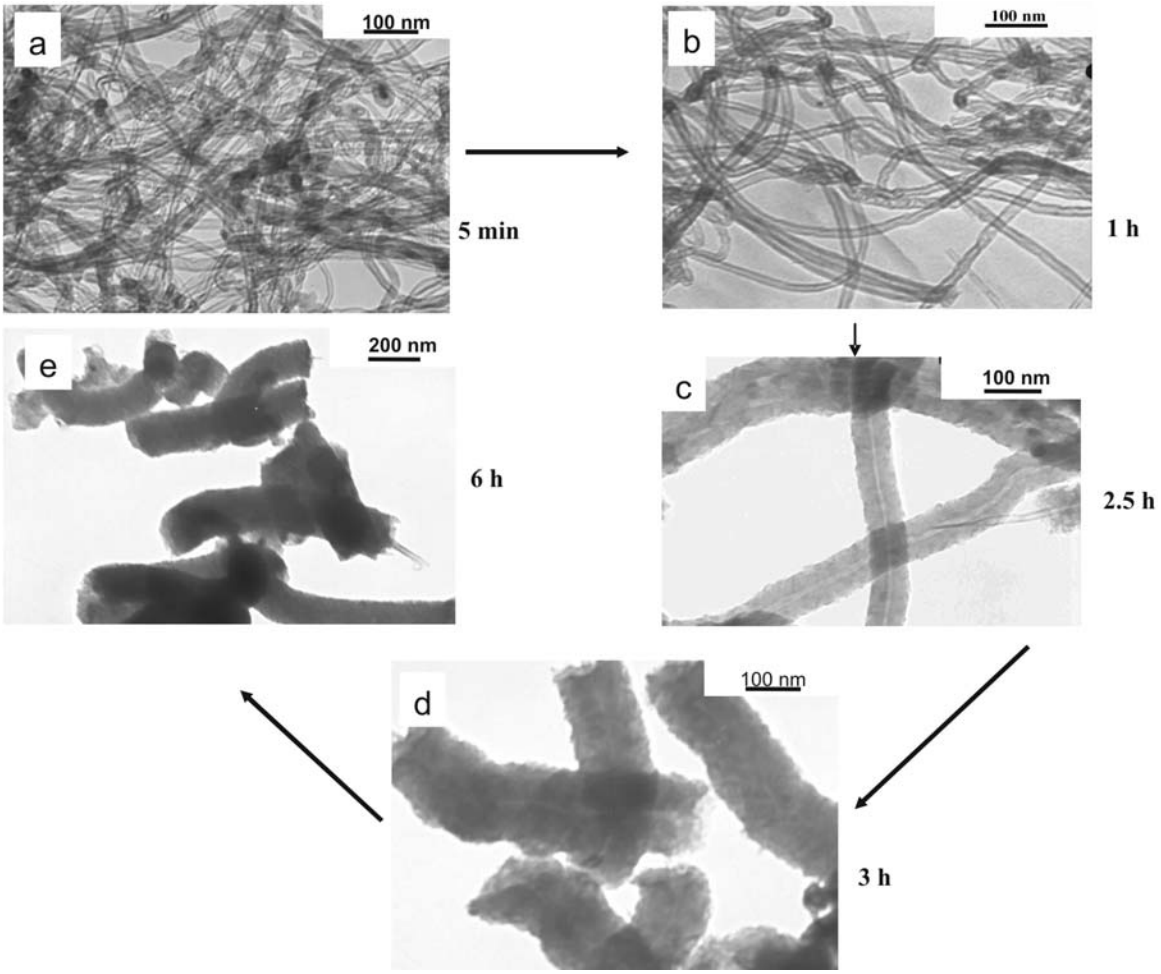

Figure 9 Low magnification TEM images of impure CNTs produced after (**a**) 5 min, (**b**) 1 h, (c) 2.5 h, (**d**) 3 h, and (**e**) 6 h reaction time at 700 °C using IMPN catalysts.

(Fig. 9c). After 3 and 6 h the tubes were even shorter and thicker and had a fibre-like morphology (Figs. 9d and 9e). These materials were coarser, with a sand-like texture. It can thus be seen that the quality of the CNTs deteriorated with time. This change in quality of the CNTs relates to the deposition of carbon on the already formed CNTs[33] and also fragmentation of the tubes. It appears that the presence of the catalyst on the $CaCO_3$/CaO at the high reaction temperature results in tube cleavage. To our knowledge there are no reports in the literature in which carbon nanotubes have been reported to be broken by the procedures described, although there is precedent for carbon deposition on fibres and tubes.[40]

Also of note is the observation that the outer diameters of the CNTs increased with increase in synthesis time while the inner diameters (~ 10 nm) were not affected (Fig. 10). Clearly shorter synthesis times (t < 60 min) result in higher quality CNTs with higher aspect ratios compared with longer times (e.g. t > 60 min).

To verify the observation that the CNTs broke into smaller pieces due to the deposition of carbon, CNTs (100 mg) synthesized for 5 min and 1 h were purified by washing in 30 % HNO_3 for 3 h to remove the Fe-Co catalyst and the support. The CNTs were then placed in a quartz boat in a reactor that was heated to 700 °C under N_2 (40 mL min^{-1}). A 1:3 C_2H_2 and N_2 gas mixture was then passed over the CNTs for periods of 3 h and 6 h, respectively. TEM images revealed that these CNTs were similar to those shown in Figs. 9d and 9e. Thus the tubes were thickened and broken by the deposition of carbon on the pre-prepared CNTs.

3.5. Purification of CNTs

A TGA study revealed that the as-synthesized carbon material contained residue (Fe-Co and CaO). To purify the CNTs, 30 % nitric acid (HNO_3) solution was used. The product was stirred in an excess amount of the acid for 30 h and for 3 days at room temperature and then washed with distilled water until neutral. In another procedure the samples were stirred in an excess

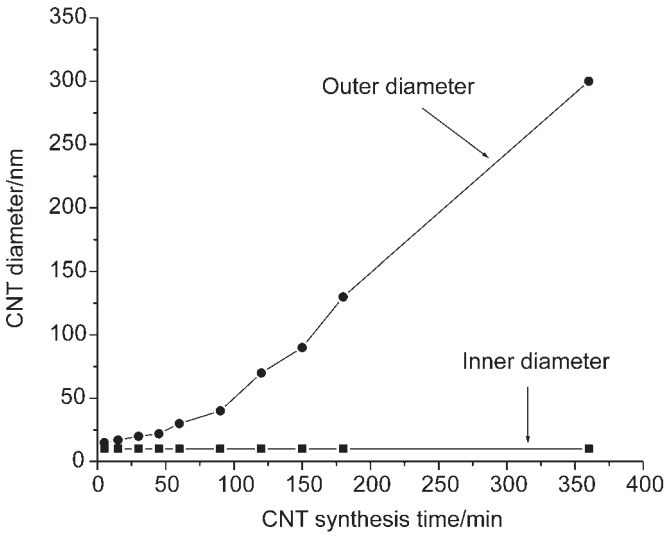

Figure 10 A plot of variation of the CNT diameter with time for CNTs synthesized over IMP Fe-Co/$CaCO_3$ catalysts.

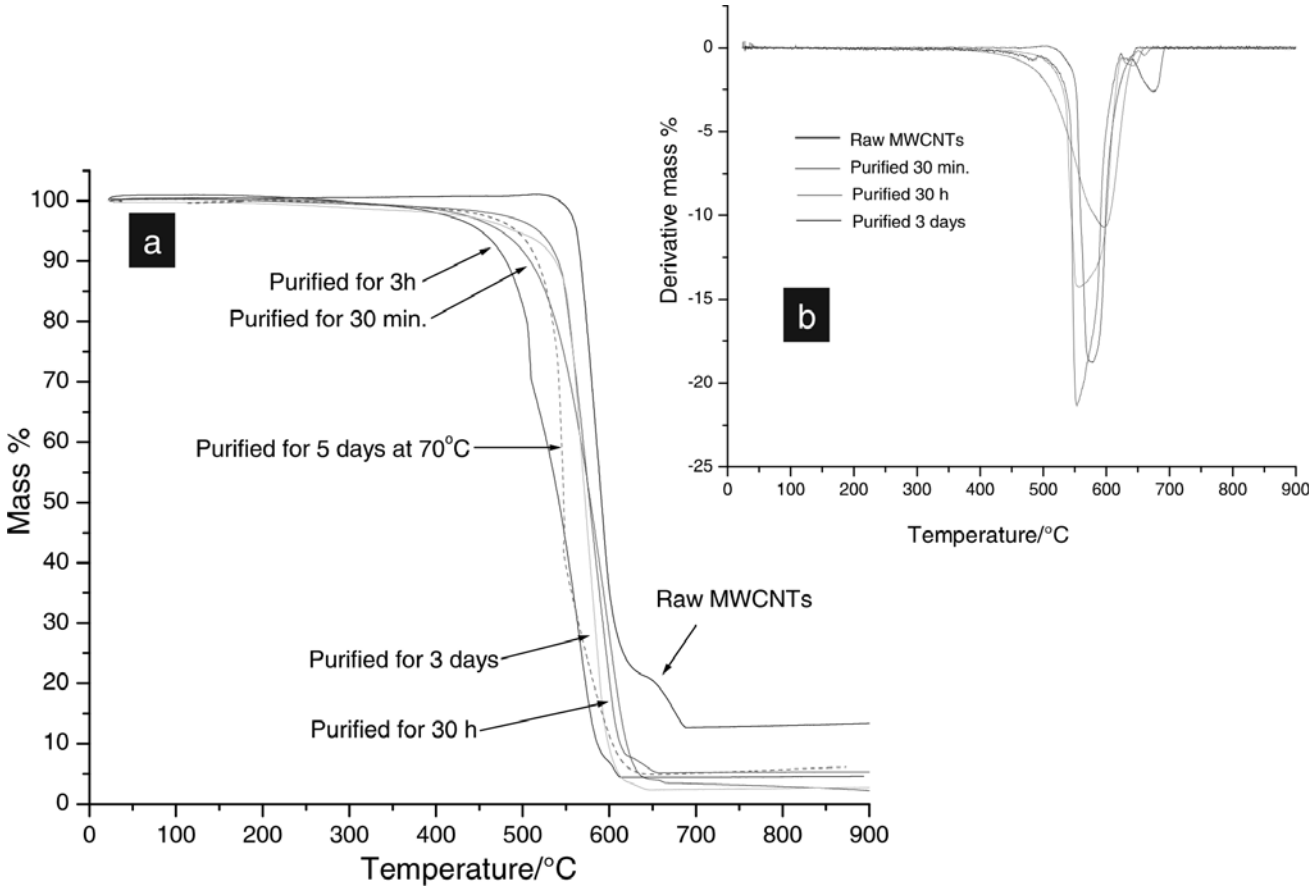

Figure 11 TGA profiles of (**a**) crude and purified CNTs synthesized from IMPN catalysts and (**b**) corresponding derivative profiles.

HNO_3 solution for 5 h and rinsed with distilled water every 30 min. Small samples were removed after the 30 min washings, dried and analyzed by TGA.

The CNTs prepared by the IMP and DP contained less residual substrate (CaO) and metal particles in the final product (~12 and 15 %, respectively) than the CNTs prepared by the RM method. This related to the lower yield of CNTs formed in this reaction. The TGA profiles of the CNTs show that all the unpurified catalysts are thermally stable up to 550 °C, where oxidation of carbon begins to occur (Fig. 11). At temperatures >550 °C only the CaO and possibly some Fe-Co catalyst remains. After acid treatment, the amount of residue remaining was reduced to between 3 and 6 % (Fig. 11a). The data show that washing the CNTs in acid for 30 min is sufficient to remove most of the support and metal particles. Clearly some CaO and Fe-Co is not removable despite the different acid treatment conditions. The derivative mass curves also show the presence of shoulder peaks at around 650 °C (Fig. 11b). These peaks are attributed to the decomposition of other materials such as graphitic soot.[31]

TEM analysis revealed that there was no significant impact of the acid treatment on the CNT structure. The CNTs possessed similar widths and lengths even after purification. The efficacy of the purification process was also verified by PXRD analysis, which revealed removal of the CaO (<1 % detected) (Supplementary Material Fig. S4).

4. Conclusions

High-quality MWCNTs have been synthesized in excellent yields using three different catalyst preparation methods. Parametric studies using Fe, Co and Fe-Co bimetallic catalysts supported on $CaCO_3$ and prepared by a wet impregnation method reveal that the production of CNTs from C_2H_2 is affected by the temperature, gas flow rate and synthesis time. The different synthesis methods generated CNTs with similar sizes and physical properties when the catalyst particles were of the same size. The Fe-Co bimetallic catalysts showed the best activity and near 100 % selectivity to CNTs can be observed under optimal reaction conditions. In particular, short CNT synthesis times ($t < 1$ h) resulted in good quality CNTs with smaller diameters and higher aspect ratios whereas long reaction times resulted in fragmentation of the CNTs that had thick rod/fibre-like structures. By varying the synthesis time, the outer diameters of the CNTs could be varied between 10 and 300 nm. Similar results were obtained for Fe-Co catalysts prepared by the deposition-precipitation method.

The CNTs were purified using 30 % HNO_3. The $CaCO_3$ support as well as catalyst particles were removed without affecting their CNT wall structures. Some residual material (~3 %) appears to be left behind after the washing. Studies to investigate methods to remove these residual materials and the effect on the CNT properties are under way.

Acknowledgements

We gratefully acknowledge financial support from the National Research Foundation, Mellon Postgraduate Mentoring Scheme, the CSIR and the University of the Witwatersrand. We also thank Mr Rudolf Erasmus for his assistance with Raman spectral collection and analysis.

References

1 S. Iijima, *Nature,* 1991, **354**, 56–66.
2 S. Iijima, *Physica B,* 2002, **323**, 1–5.
3 B.M. Endo, T. Hayashi, Y.A. Kim, M. Terrones and M.S. Dresselhaus, *Phil. Trans. Roy. Soc. London, A,* 2004, **362**, 2223–2238.
4 P. Ball, *Made to Measure: New Materials for the 21st Century,* Princeton

University Press, Princeton, NJ, USA, 1997.

5 M. Terrones, A. Jorio, M. Endo, Y.A. Kim, T. Hayashi, H. Terrones, J.-C. Charlier, G. Dresselhaus and M.S. Dresselhaus, *Mater. Today,* 2004, **7**, 30–45.

6 H. Zeng, L. Zhu, G. Hao and R. Sheng, *Carbon,* 1998, **36**, 259–261.

7 Z.J. Shi, Y.F. Lian, X.H. Zhou, Z.N. Gu, Y. Zhang, S. Iijima, L. Zhou and K.T. Yue, *Carbon,* 1999, **37**, 1449–1453.

8 A. Thess, R. Lee, P. Nikolaev, H. Dai, P. Petit, J. Robert, C. Xu, Y.H. Lee, S.G. Kim, A.G. Rinzler, D.T. Colbert, G.E. Scuseria, D. Tombnek and J.E. Fischer, *Science,* 1996, **273**, 483–487.

9 D.C. Li, L. Dai, S. Huang, A.W.H. Mau and Z.L. Wang, *Chem. Phys. Lett.,* 2000, **316**, 349–355.

10 V. Ivanov, J.B. Nagy, P. Lambin, A. Lucas, X.B. Zhang, X.F. Zhang, D. Bernaerts, G. Van Tendeloo, S. Amelinckx and J. Van Landuyt, *Chem. Phys. Lett.,* 1994, **223**, 329–335.

11 R. Brukh and S.C. Mitra, *Chem. Phys. Lett.,* 2006, **424**, 126–132.

12 K. Hernadi, A. Fonseca, J.B. Nagy, D. Bernaerts, J. Riga and A. Lucas, *Synthetic Metals,* 1996, **77**, 31–34.

13 K. Hernadi, Z. Kónya, A. Siska, J. Kiss, A. Oszkó, J.B. Nagy and I. Kiricsi, *Mat. Chem. Phys.,* 2002, **77**, 536–541.

14 A.L. Balch and M.M. Olmstead, *Chem. Rev.,* 1998, **98**, 2123–2166.

15 K. Hernadi, A. Fonseca, J.B. Nagy, A. Fudala, D. Baenaerts and A. Lucas, *Zeolites,* 1996, **17**, 416–423.

16 P. Francesco, *Catal. Today,* 1998, **41**, 129–137.

17 E. Couteau, K. Hernadi, J.W. Seo, L. Thiên-Nga, C. Mikó, R. Gaá1 and L. Forró, *Chem. Phys. Lett.,* 2002, **378**, 9–17.

18 H. Kathyayini, N. Nagaraju, A. Fonseca and J.B. Nagy, *J. Mol. Catal.,* 2004, **223**, 129–136.

19 M.C. Bahome, L.L. Jewell, D. Hildebrandt, D. Glasser and N.J. Coville, *Appl. Catal. A: General,* 2005, **287**, 60–67.

20 J. Cheng, X. Zhang, Z. Luo, F. Liu, Y. Ye, W. Yin, W. Liu and Y. Han, *Mat. Chem. Phys.,* 2006, **95**, 5–11.

21 A. Magrez, J.W. Seo, C. Mikó, K. Hernádi and L. Forro, *J. Phys. Chem. B,* 2005, **109**, 10087–10091.

22 A. Magrez, J.W. Seo, V.L. Kuznetsov and L. Forró, *Angew. Chem. Int. Ed. Engl.,* 2007, **46**, 441–444.

23 P. Serp, M. Cossias and P. Kalck, *Appl. Catal. A: General,* 2003, **253**, 337–358.

24 Z. Yu, D. Chen, B. Tøtdal and A. Holmen, *Catal. Today,* 2005, **100**, 261–267.

25 A.-C. Dupuis, *Prog. Mat. Sci.,* 2005, **50**, 17–20.

26 W. Qian, T. Liu, Z. Wang, H. Yu, Z. Li, F. Wei and G. Luo, *Carbon,* 2003, **41**, 2487–2493.

27 B. Louis, G. Gulino, R. Vieira, J. Amadou, T. Dintzer, S. Galvagno, G. Centi, M.J. Ledoux and C. Pham-Huu, *Catal. Today,* 2005, **102–103**, 23–28.

28 G. Che, B.B. Lakshmi, C.R. Martin and E.R. Fisher, *Chem. Mater.,* 1998, **10**, 260–267.

29 E. Dervishi, Z. Li, A.R. Biris, D. Lupu, S. Trigwell and A.S. Biris, *Chem. Mater.*, 2007, **19**, 179–184.

30 T.C. Schmitt, A.S. Biris, D.W. Miller, A.R. Biris, D. Lupu, S. Trigwell and Z.U. Rahman, *Carbon,* 2006, **44**, 2032–2038.

31 C.H. See and A.T. Harris, *Particle Tech. Fluidization,* 2008, **54**, 657–664.

32 (a) M. Boutonnet, J. Kizling and P. Stenius, *Colloids and Surfaces,* 1982, **5**, 209–225; (b) E.E. Carpenter, *J. Magnetism Magnetic Mater.,* 2001, **225**, 17–20; (c) C.T. Seip and C.J. O'Connor, *Nanostr. Mater.,* 1999, **12**, 183–186; (d) I. Ban, M. Drofenik and D. Makovec, *J. Magnetism Magnetic Mater.,* 2006, **307**, 250–256; (e) Y. Lee, J. Lee, C.J. Bae, J.-G. Park, H.-J. Noh, J.-H. Park and T. Hyeon, *Adv. Funct. Mater.,* 2005, **15**, 503–509; (f) V. Pillai, P. Kumar, M.S. Multani and D.O. Shah, *Colloids and Surfaces A: Physicochem. Eng. Aspects,* 1993, **80**, 69–75.

33 M. Escober, M.S. Moreno, R.J. Candal, M.C. Marchi, A. Caso, P.I. Polosecki. G.H. Rubiolo and S. Goyanes, *Appl. Surf. Sci.*, 2007, **254**, 251–256.

34 (a) A. Zhang, C. Li, S. Bao and Q. Xu, *Microp. Mesop. Mater.,* 1999, **29**, 383–388; (b) J.-B. Park, G.-S. Choi, Y.-S. Cho, S.-Y. Hong, D. Kim, S.-Y. Choi, J.-H. Lee and K.-I. Cho, *J. Cryst. Growth,* 2002, **244**, 211–217; (c) C. Emmenegger, P. Mauron, A. Züttel, C. Nützenadel, A. Schneuwly, R. Gallay and L. Schlapbach, *Appl. Surf. Sci.,* 2000, **162–163**, 452–456.

35 S.D. Mhlanga and N.J. Coville, *Diam. Rel. Mater.,* 2008, **17**, 1489–1493.

36 A. Jorio, M.A. Pimenta, A.G.S. Filho, R. Saito, G. Dresselhaus and M.S. Dresselhaus, *New J. Phys.,* 2003, **5**, 139.1–139.17.

37 Z.L. Wang and Z.C. Kang, *J. Phys. Chem.,* 1996, **100**, 5163–5165.

38 V.G. Pol, M. Motiei, A. Gedanken, J. Calderon-Moreno and M. Yoshimura, *Carbon,* 2004, **42**, 111–116.

39 http://www.carbonblack.jp/en/cb/youto.html#top. Accessed 1 June 2007.

40 M. Monthioux, H. Allouche and R.L. Jacobsen, *Carbon,* 2006, **44**, 3183–3194.

Supplementary material to:

S.D. Mhlanga, K.C. Mondal, R.Carter, M.J. Witcomb and N.J. Coville, *S. Afr. J. Chem.,* 2009, **62**, 67–76.

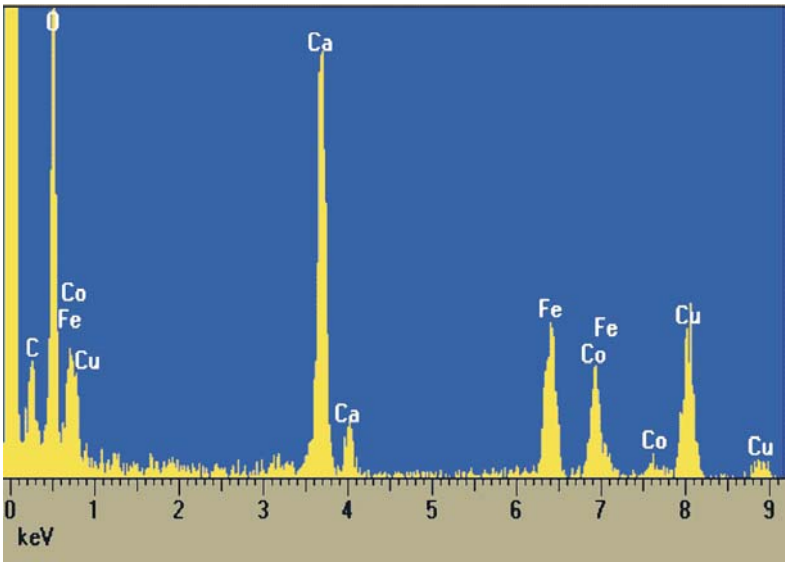

Figure S1 An EDX spectrum of IMPN indicating the presence of Fe-Co nanoparticles.

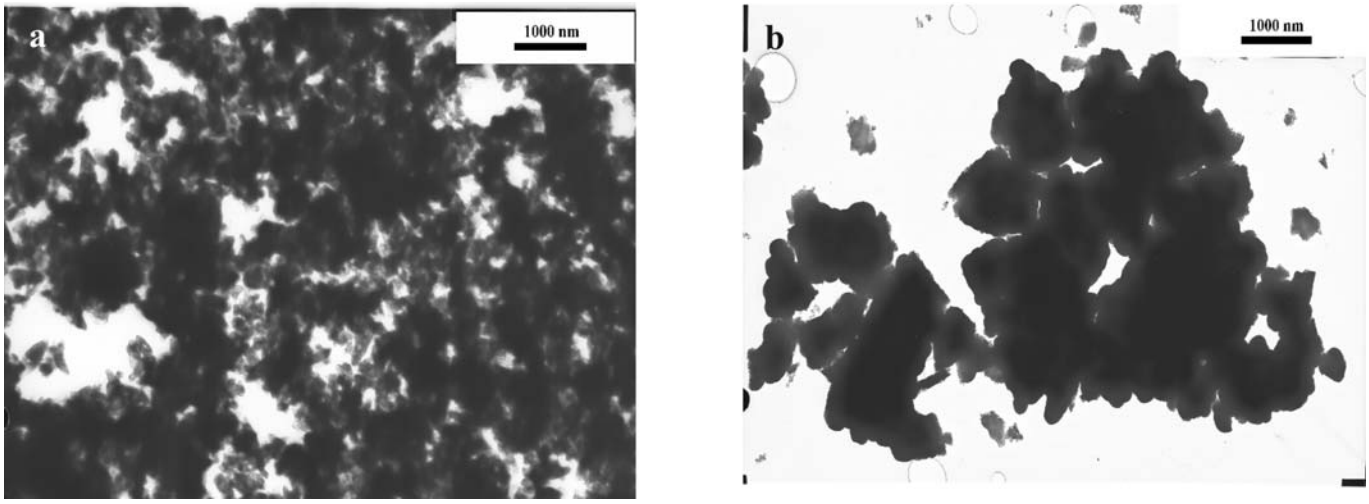

Figure S2 TEM images of $CaCO_3$ heated at 700 °C under C_2H_2 for (**a**) 1 h and (**b**) 6 h.

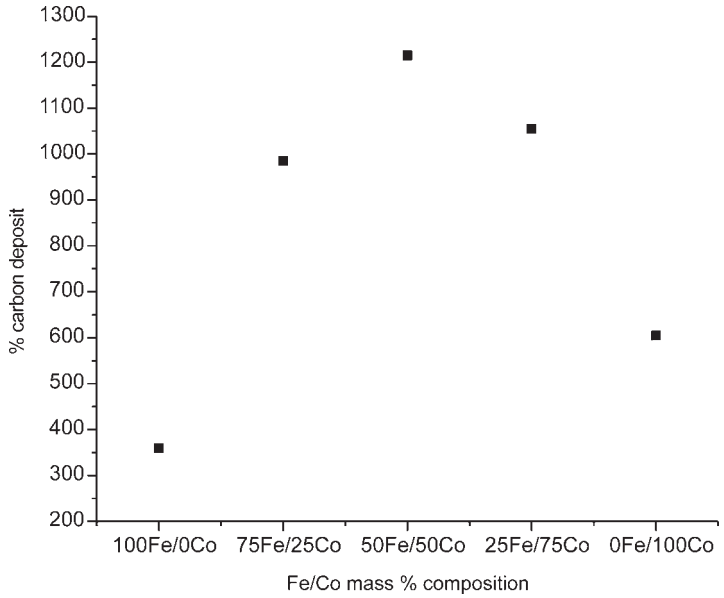

Figure S3 Amount of carbon deposit produced using 5 mass % Fe-Co/$CaCO_3$ with different amounts of Fe and Co in the alloy.

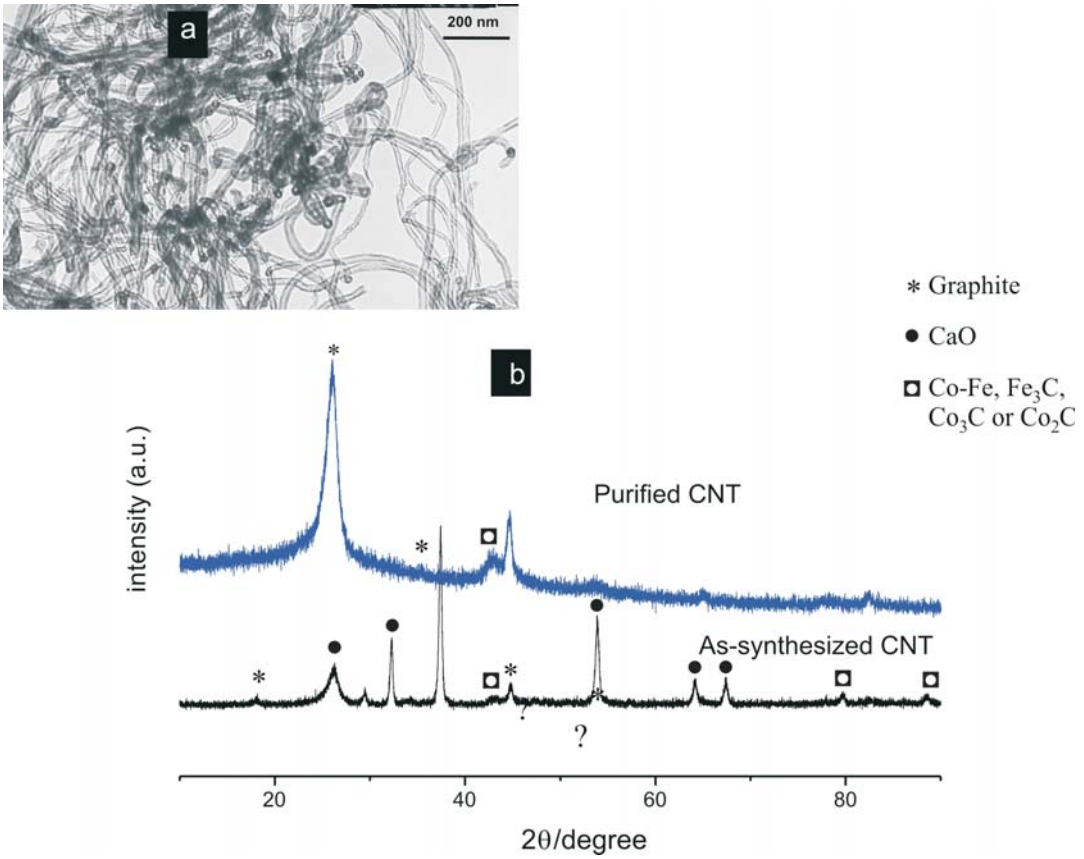

Figure S4 (**a**) A TEM image of purified CNTs and (**b**) a PXRD pattern of the purified and as-synthesized (raw) CNTs